Incised valley paleoenvironments interpreted by seismic stratigraphic approach in Patos Lagoon, Southern Brazil

DOI: 10.1590/2317-4889201820170133

ARTICLE

Incised valley paleoenvironments interpreted by seismic stratigraphic approach in Patos Lagoon, Southern Brazil

Eduardo Calixto Bortolin[1*], Jair Weschenfelder[1,2], Andrew Cooper[3,4]

ABSTRACT: *The Rio Grande do Sul (RS) coastal plain area (33,000 km²) had its physiography modified several times through the Quaternary, responding to allogenic and autogenic forcings. The Patos Lagoon covers a significant area of RS coastal plain (10,000 km²), where incised valleys were identified in previous works. About 1,000 km of high resolution (3.5 kHz) seismic profiles, radiocarbon datings, Standard Penetration Test (SPT) and gravity cores were analyzed to interpret the paleoenvironmental evolution as preserved in incised valley infills. Seismic facies were recognized by seismic parameters. The sediment cores were used to ground-truth the seismic interpretations and help in the paleoenvironmental identification. Key surfaces were established to detail the stratigraphical framework, and seismic facies were grouped into four seismic units, which one classified in respective system tracts within three depositional sequences. The oldest preserved deposits are predominantly fluvial and estuarine facies, representing the falling stage and lowstand system tracts. The Holocene transgressive records are dominated by muddy material, mainly represented by estuarine facies with local variations. The transgression culminated in Late Holocene deposits of Patos Lagoon, representing the highstand system tract. The depositional pattern of the vertical succession was controlled by eustatic variations, while the autogenic forcing (paleogeography and sediment supply) modulated the local facies variation.*

KEYWORDS: *incised valley; seismic facies; Quaternary; system tracts.*

INTRODUCTION

The response of coastal environments to sea-level variations has received much attention (Schumm 1993, Shanley & McCabe 1994, Blum & Törnqvist 2000). River incision across the subaerially exposed continental shelf was followed by drowning during the transgression of the last glacial cycle (Dalrymple *et al.* 1994, 2006, Blum *et al.* 2013).

The Patos Lagoon, in southern Brazil, is the biggest barrier lagoon in the world (~ 10,000 km²), with a single permanent tidal inlet in Rio Grande (Kjerfve 1994, Toldo Jr. *et al.* 2006b). Initial studies using high-resolution seismic data investigated Late Quaternary paleoenvironments in the Patos Lagoon (Weschenfelder *et al.* 2006, 2010a, 2014), whose results established a general and regional geological framework.

This study provides an individualization of seismic units, with a more detailed facies description, allowing the interpretation of system tracts and correlation with the regional sea level curve. The aims are to understand paleovalley formation and subsequent evolution, and to investigate their role in postglacial evolution of the Patos Lagoon system.

Regional setting

Rio Grande do Sul state (RS) is located between 29º and 34º south (Fig. 1). It has a wide and low relief coastal plain (0.03º–0.08º slope). During the Quaternary, transgressive-regressive cycles reworked alluvial fans and shelf sediments, creating four barrier/lagoon systems that are preserved on the coastal plain. These sandy barriers are named, from

[1]Programa de Pós-Graduação em Geociências, Instituto de Geociências, Universidade Federal do Rio Grande do Sul – Porto Alegre (RS), Brazil.
E-mail: eduardo_bortolin_22@hotmail.com

[2]Centro de Estudos de Geologia Costeira e Oceânica, Instituto de Geociências, Universidade Federal do Rio Grande do Sul – Porto Alegre (RS), Brazil.
E-mail: jair.weschenfelder@ufrgs.br

[3]School of Geography & Environmental Sciences, Environmental Sciences Research Institute, Ulster University – Coleraine, Co. Londonderry, Northern Ireland.
E-mail: jag.cooper@ulster.ac.uk

[4]School of Agriculture, Earth and Environmental Sciences, University of KwaZulu-Natal – Durban, South Africa.

*Corresponding author

Manuscript ID: 20170133. **Received on:** 11/10/2017. **Approved on:** 08/03/2018.

oldest to youngest, as Barriers I, II, III, and IV (Villwock *et al.* 1986). Barrier III is the youngest Pleistocene barrier, which deposits are related to Marine Isotope Stage (MIS) 5 and it, together with the Holocene barrier (IV), encloses the contemporary Patos Lagoon.

The Patos Lagoon is oriented NE-SW. It is about 240 km long, with average width of 40 km, and the surface area is ~ 10,000 km^2 (Kjerfve 1986, Toldo Jr. *et al.* 2006b). The single permanent connection with the ocean is the Rio Grande channel, and the tidal range average in the lagoon is about

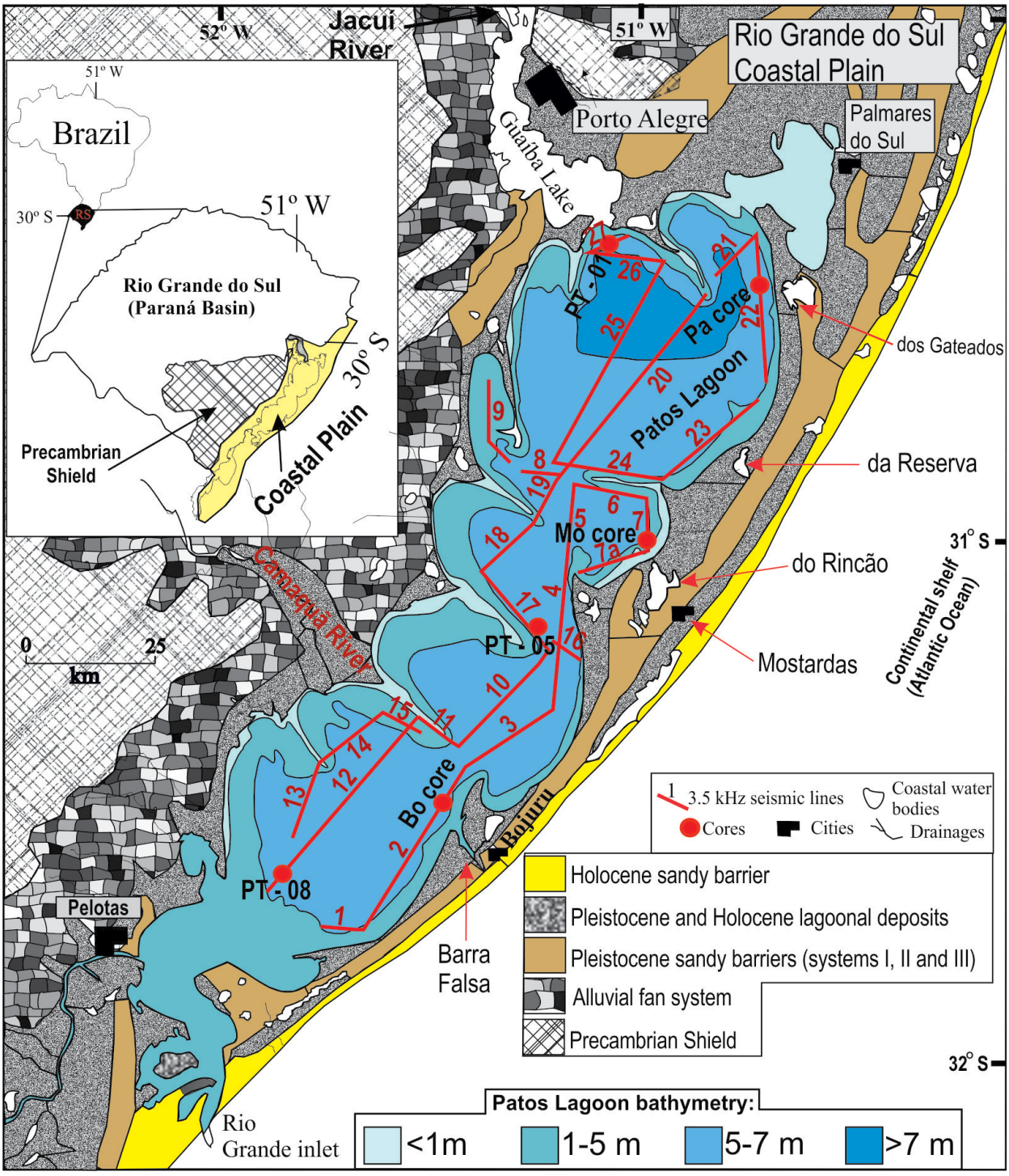

Figure 1. Regional setting with geological mapping, bathymetry of Patos Lagoon, toponymies, seismic profiles and core locations, modified from Bortolin *et al.* (2018). Coastal plain geology based on Tomazelli & Villwock (2000). Patos Lagoon bathymetry from Corrêa (1996) and Toldo Jr. *et al.* (2000).

0.22 m (DHN, 2014). The lagoon receives freshwater of two main drainage basins: Jacuí/Guaíba Rivers, in the north, and Camaquã River, in the south (Marques 2005). These rivers are the main source of sediment into the lagoon. Several morphologic and hydrodynamic cells, partially separated by sandy spits, are present in the Patos Lagoon. The segmentation process, as proposed by Zenkovitch (1959), is believed to be incomplete because of currents associated with freshwater influx (Toldo Jr. 1991). The submerged relief of each lagoonal cell comprises two sections: the margins (< 5 m water depth) are mainly sandy deposits, over which grow sandy spits in water depths of circa 1 m depth; the central portion of the cells have an average depth about 6 m, and the deposits are mainly muddy sediments (Toldo Jr. 1991, Toldo Jr. *et al*. 2006b).

Paleodrainage systems and related features were identified in the lagoon during a seismic reflection survey (Weschenfelder *et al*. 2005; Weschenfelder *et al*. 2010a), as well on the adjacent continental shelf (Abreu & Calliari 2005). Weschenfelder *et al*. (2005) developed the first stratigraphic sequence approach, with a provisional seismic facies description, based basically on the internal configuration pattern of reflectors mapped on seismic line 2 (Fig. 1), but this previous study did not associate a specific facies with an individual paleoenvironment. An inland core was drilled in the landward projection of the paleochannel associated to Barra Falsa; it provided samples for multidisciplinary research involving lithology, palynomorph and diatom data. That study aimed to interpret the paleoenvironmental evolution of the paleochannel recognized by seismic data in seismic line 2 (Weschenfelder *et al*. 2008b).

Two Pre-Holocene phases of incision were identified by the mapping of unconformity surfaces, and by the relative position in the sedimentary sequence and by radiocarbon dates (Weschenfelder *et al*. 2005, 2010a, 2014). These incisions probably occurred during the Pleistocene, reaching its maximum during the maximum regression of the Wisconsin Glaciation (Weschenfelder *et al*. 2010a, 2014). The upper paleodrainage systems recognized were formed during sea level fall of the Last Glacial Maximum (LGM), when the sea level was 120/130 m below the actual position and were infilled during Holocene. From 18,000 years BP, postglacial sea level rise caused paleovalleys drowning and infilling (Corrêa 1986, Weschenfelder *et al*. 2008a, 2008b, 2010a, 2014, 2016).

Previous studies suggest the breaching of the Pleistocene Barrier III (Toldo Jr. *et al*. 1991, Barboza *et al*. 2005, Weschenfelder *et al*. 2008b, 2014, Santos-Fischer *et al*. 2016, 2018). The pioneer study relating a feature named Barra Falsa in the eastern Patos Lagoon margin to a Holocene inlet was carried out by Toldo Jr. *et al*. (1991). Following, few studies based on seismic stratigraphic, palynomorph and diatom analysis also corroborated this interpretation (Weschenfelder *et al*. 2008b, 2014, Santos-Fischer *et al*. 2016, 2018, Bortolin 2017, Bortolin *et al*. 2018). Besides Barra Falsa, other features in the Patos Lagoon eastern margin, such as Rincão Lake, Reserva Lake and Gateados Lake (Fig.1), also could be indicative of Holocene inlets (Bortolin 2017; Bortolin *et al*. 2018).

Jacuí and Camaquã rivers were responsible for excavating the main paleovalleys recognized in Patos Lagoon substrate, developing different waterways during the Pleistocene (Weschenfelder *et al*. 2010a, 2014, Baitelli 2012, Bortolin 2017). The valleys developed were partially infilled and are still recognizable in the Patos Lagoon bathymetry (Bortolin 2017; Bortolin *et al*. 2018).

MATERIALS AND METHODS

About 1,000 km of high-resolution (3.5 kHz) seismic profiles were collected in the Patos Lagoon (Fig. 1), aboard the research vessel LARUS. Positioning was by differential global positioning system (DGPS). The data was acquired by a GeoPulse Sub Bottom Profiler, from GeoAcoustics (Great Yarmouth, United Kingdom), and was processed in SonarWiz software (Chesapeake Technology, California, United States). These seismic data were analyzed in previous works with distinct approaches, but still provide a unique source of information and are necessary to support our interpretations (Weschenfelder *et al*. 2005, 2006, 2008a, 2008b, 2010a, 2010b, 2014, 2016). Average velocities applied were 1,500 m/s for the water and 1,650 m/s for sediments (Jones 1999).

The concepts established by Mitchum *et al*. (1977) were applied to limit the depositional sequence, to define the seismic units and to describe the parameters of each facies. Throughout this work, the generic term *discontinuity* is applied to the surfaces, each of which represents a break in the continuity of physical character, either by contrast in acoustic impedance or the geometric relationship between strata. The term *unconformity* is applied to the sequence boundaries, specifically when a hiatus or erosion is identified.

The criteria used to differentiate seismic units are the same as those used to separate the depositional sequence into stratigraphic units (system tracts): strata stratification patterns (internal configuration of reflectors), position within the sequence, and types of bounding surface (Catuneanu 2006, Catuneanu *et al.* 2011). Therefore, in this work seismic units are relative to a specific system tract.

Seismic facies were identified by seismic parameters, such as amplitude, frequency, continuity of the reflections,

internal configuration, external geometry, and irrespective of position in the depositional sequence. Seismic facies were used as a tool to interpret the paleoenvironment based on James & Dalrymple (1992). Accordingly, a specific seismic facies (paleoenvironment) could occur in distinct system tracts (stratigraphic/seismic units).

Contrasting acoustic impedance surfaces were minutely described. Care was taken to disregard multiples and also "bottom simulating reflectors" (Emery & Myers 1996), which can be produced in zones with gas in the sediment. The continuity of some seismic surfaces was obliterated by gas-related acoustic anomalies in some locations.

A stratigraphic calibration was carried out using sediment cores after the seismic interpretation. Three Standard Penetration Test (SPT) boreholes, located exactly on the seismic profiles, were analyzed. In addition, three gravity cores of 3 m average length were collected. Shells were selected for radiocarbon dating (C^{14}), to establish the age of some units and to correlate them with the stratigraphic framework (Tab. 1). Some of the radiocarbon ages presented in Table 1 were published by previous works, but the shell species were not reported (Santos-Fischer *et al.* 2016, Weschenfelder *et al.* 2014). Radiocarbon ages with the corresponding species were published by Baitelli (2012),

Table 1. References of cores and radiocarbon dating samples published previously and in the current work, modified from Bortolin *et al.* (2018). Compilation of shell species with organized references.

Core/samples/ depths	Geographical coordinate	Calibrated ages BP	Material	Species	Sample	Publication
Bo core (-8 m water clomun)						
Bo 12 (4 m)	31º31'30" S 51º29'50" W	7535 ± 105 (7640/7430)	Shell	*Ostrea equestris*	BETA 294867	Baitelli 2012, Weschenfelder *et al.* 2014
Bo 15 (7 m)		7790 ± 140 (7930/7650)	Shell	*Heleobia australis*	BETA 359870	Santos-Fischer *et al.* 2016
Bo 19 (11 m)		7875 ± 115 (7990/7760)	Shell	*Heleobia australis*	BETA 294868	Baitelli 2012, Weschenfelder *et al.* 2014
Bo 20 (12 m)		8010 ± 140 (8150/7870)	Shell	Shell fragments	BETA 359871	Santos-Fischer *et al.* 2016
Mo core (-7.30 m water column)						
Mo 8 (0.70 m)	31º00'25" S 51º00'10" W	7820 ± 140 (7960/7680)	Shell	*Erodona Mactroides*	BETA 360370	Santos-Fischer *et al.* 2016, Dehnhardt 2017
Mo 11 (3.7 m)		7865 ± 115 (7980/7750)	Shell	*Clausinella gayi*	BETA 298208	Baitelli 2012, Weschenfelder *et al.* 2014, Dehnhardt 2017
Mo 13 (5.7 m)		8040 ± 120 (8160/7920)	Shell	*Clausinella gayi*	BETA 294869	Baitelli 2012, Weschenfelder *et al.* 2014, Dehnhardt 2017
Pa core (-6 m water column)						
Pa 21 (15 m)	30º32'52" S 50º42'54" W	> 43,500	Shell	*Nucula semiornata*	BETA 305998	Baitelli 2012, Weschenfelder *et al.* 2014
Pa 23 (17 m)		> 43,500	Shell	*Nucula semiornata*	BETA 305999	Baitelli 2012, Weschenfelder *et al.* 2014
Pa 26 (20 m)		> 43,500	Shell	*Nucula semiornata*	BETA 298209	Baitelli 2012, Weschenfelder *et al.* 2014
PT-08 (-6 m water column)						
PT-08 (0.60 m)	31º39'56" S 51º53'24" W	4747 ± 98 (4845/4649)	Shell	not recognized	BETA 453296	Bortolin 2017, Bortolin *et al.* 2018
PT-05 (-6m water column)	31º11'09" S - 51º17'17" W	no samples dated	unavailable	unavailable	unavailable	Bortolin 2017, Bortolin *et al.* 2018
PT-01 (-6m water column)	30º25'54" S- 51º04'46" W	no samples dated	unavailable	unavailable	unavailable	Bortolin 2017, Bortolin *et al.* 2018

and the species nomenclature was reviewed by Dehnhardt (2017). These data were compiled in the current work and organized in Table 1.

Provisional descriptions of seismic facies were developed in earlier studies (Weschenfelder *et al.* 2005, 2008b, 2010a), which focused basically on the paleochannel in the northern portion of seismic line 2, near the Bojuru region. Those works described channel infilling facies, but did not apply a uniform nomenclature to the facies. Seismic facies were described by Weschenfelder et al. (2005, 2010a) without paleonvironment interpretation, while Weschenfelder *et al.* (2008b) associated the facies to paleoenvironments. Considering the previous studies, the current work standardizes the nomenclature of facies, key surfaces, and sequences, extending this model to all recognizable features in the Patos Lagoon seismic data. Based on this, it provides a more consistent interpretation about the environmental evolution in the whole Patos Lagoon area.

RESULTS

The acoustic signal penetrated about 30 m of sediment, encompassing the upper sedimentary package underneath the Patos Lagoon bottom. Three depositional sequences were identified, limited by subaerial unconformities (SU and SU1). The lowest sequence (S1) reveals multiple events of incision and subsequent infilling of the valleys. These are the oldest events recorded. The upper sequences (S2 and S3) reflect evolution from the peak of the Last Full Interglacial (LFI), isotope stage 5e (about 120 ky BP), to the present. Figure 2 synthesizes this stratigraphic framework.

Sequence 1 (S1) is the deepest recognized in the seismic data. The lower limit was not reached by the seismic signal. The upper limit is at an average depth of 17 m below the water level (6 m on average), and it is marked by a discontinuity surface, named here SU (Figs. 2, 3, 4, 5, 6), that truncates older strata. S1 reveals multiple reflectors, with parallel to sub-parallel configuration, good lateral continuity and variable amplitude. This sequence was first recognized by Weschenfelder *et al.* (2005), and named Sequence I, identifying it in seismic line 2 (Fig. 1). Subsequent seismic studies used the same terminology (Weschenfelder *et al.* 2010a, 2014, Baitelli 2012, Santos-Fischer *et al.* 2016, 2018, Bortolin 2017, Bortolin *et al.* 2018).

The lower and upper limits of Sequence 2 (S2) are limited by discontinuity surfaces, SU and SU1, which have similar seismic parameters (described ahead), but SU1 is topping younger deposits and has a lower truncation angle with older strata (Fig. 6). The lower limit of S2 is marked by SU, with truncation of S1 deposits (Figs. 3, 4, 5, 6). The upper limit is marked by SU1 (Fig. 6), a very irregular and high amplitude surface, truncating in low angle the deposits of S2 strata, and small channels (< 2 m) can be recognized in this surface. This sequence is composed of Facies A, B and C of Unit 1 (Fig. 2).

The limits of Sequence 3 (S3) are well marked on the base by an unconformity surface, SU or SU1, depending on whether Unit 1 deposits were eroded or not deposited, and on the top by the Patos Lagoon floor. When Unit 1 deposits are not recorded SU and SU1 surfaces are juxtaposed and are represented as only as SU. This sequence represents the post-LGM transgressive infilling event. Weschenfelder *et al.* (2005, 2010a) described a few channel infilling facies of this sequence, in seismic line 2, associated with Bojuru paleochannel (Fig. 1).

Seismic facies

Seismic facies were identified by seismic parameters, such as amplitude, frequency, continuity of the reflections, internal configuration and external geometry. Sedimentologic samples were tied to seismic data. Besides the classic parameters, the presence of gas also can be used to suggest the presence of some paleoenvironments (Weschenfelder *et al.* 2016).

Facies A (Figs. 2, 5, 6) comprises a 6 m-thick package of confined channel infilling reflectors, whose cross-sectional shape is concave upward. The reflectors are semi-transparent, with low amplitude, low layering, inclined, low continuity and high frequency. Sometimes a switch of pattern is distinguishable around the middle portion of the fluvial sedimentary package. This change determines the beginning of Facies B (Figs. 2, 5, 6), in which high-amplitude reflectors of medium continuity and low frequency onlap the subaerial unconformity surface. Facies A and B are interpreted as V-shaped fluvial incisions, located at the base of U-shaped incised valleys.

Facies A and B are recognized mainly by the external geometry of channel fill type. Together, they form a total package of 10 m thickness on average. The underlying strata is mainly composed of parallel/subparallel, continuous to discontinuous reflectors, which are truncated by the basal surface of Facies A and B (Weschenfelder *et al.* 2010a). The vertical accretion is symmetric, concentric and confined in a V-shaped fixed channel (Gibling 2006) with no lateral migration. The reflectors downdip toward the channel center and onlap the unconformity surface. One feature stands out in both facies: the reflectors have a geometric shift from concave upward to almost horizontal towards the top. This is particularly evident in Facies B. Two SPT cores (Bo and Pa; Figs. 2 and 5) reached these facies showing an almost homogeneous package, of alternating fine and medium sands and no fossils available for dating.

Facies C (Figs. 2 to 6) consists of a homogeneous succession with aggradational sediments. It shows reflectors with external sheet forms, low amplitude (rare exceptions), high continuity (kilometrical scale), high frequency and well-formed parallel/sub-parallel layering. The layers are horizontal in the central portion of the valleys and tend

	Unit	System tract	Seismic facies	Sediment and thickness	Depositional environment	Main diagnostic criteria	Seismic image
S3	HST	U4	G	Mud/ 0.7 m	Back- barrier lagoon	High lateral continuity. High amplitude reflectors capping the MFS.	
	MFS		F	Sand ? +- 4 m	Overspilling	High amplitude reflectors, bank external geometry, near to paleointerfluve.	
	TST	U3	E	Mud and sand +- 12 m	Inlets	Infilling geometry, aggradational/progradational wavy reflectors.	
			D	Mud and sand alternation +- 12 m	Bay-head delta	Mounded geometry, progradational and bidi-rectional reflectors.	
			C1	Sand +- 6 m	Estuary mouth-bar	Progradational reflectors deposited over estuarine deposits (facies C).	
			C	Mud/ +- 10 m	Estuarine	Homogeneous sucession of aggradational reflectors, sheet external geoemtry.	
	TS		B	Sand/ +- 5 m	Fluvial	Channel infilling geometry, high amplitude reflectors, symmetrical and concentric infilling, tending to horizontality.	
	LST	U2	A	Sand/ +- 5 m	Fluvial	Channel infilling geometry, low amplitude reflectors, symmetrical and concentric infilling.	
S2	SU1		C	Mud/ +- 10 m	Estuarine	Homogeneous sucession of aggradational reflectors, sheet external geoemtry.	
	FSST	U1	B	Sand/ +- 5 m	Fluvial	Channel infilling geometry high amplitude reflectors, symmetrical and concentric infilling, tending to horizontality.	
			A	Sand/ +- 5 m	Fluvial	Channel infilling geometry, low amplitude reflectors, symmetrical and concentric infilling.	
	SU						
S1							

S1: Sequence 1; S2: Sequence 2; S3: Sequence 3; SU: subaerial unconformity; SU1: subaerial unconformity 1; TS: transgressive surface; MFS: maximum flooding surface; FSST: falling-stage system tract; U1: Unit 1; LST: lowsand sytem tract; U2: Unit 2; TST: transgressive sytem tract; U3: Unit 3; HST: highstand system tract; U4: Unit 4.

Figure 2. Stratigraphical framework, with system tracts and seismic facies interpretations. The stratigraphical sequences individualization was based on Weschenfelder *et al.* (2014).

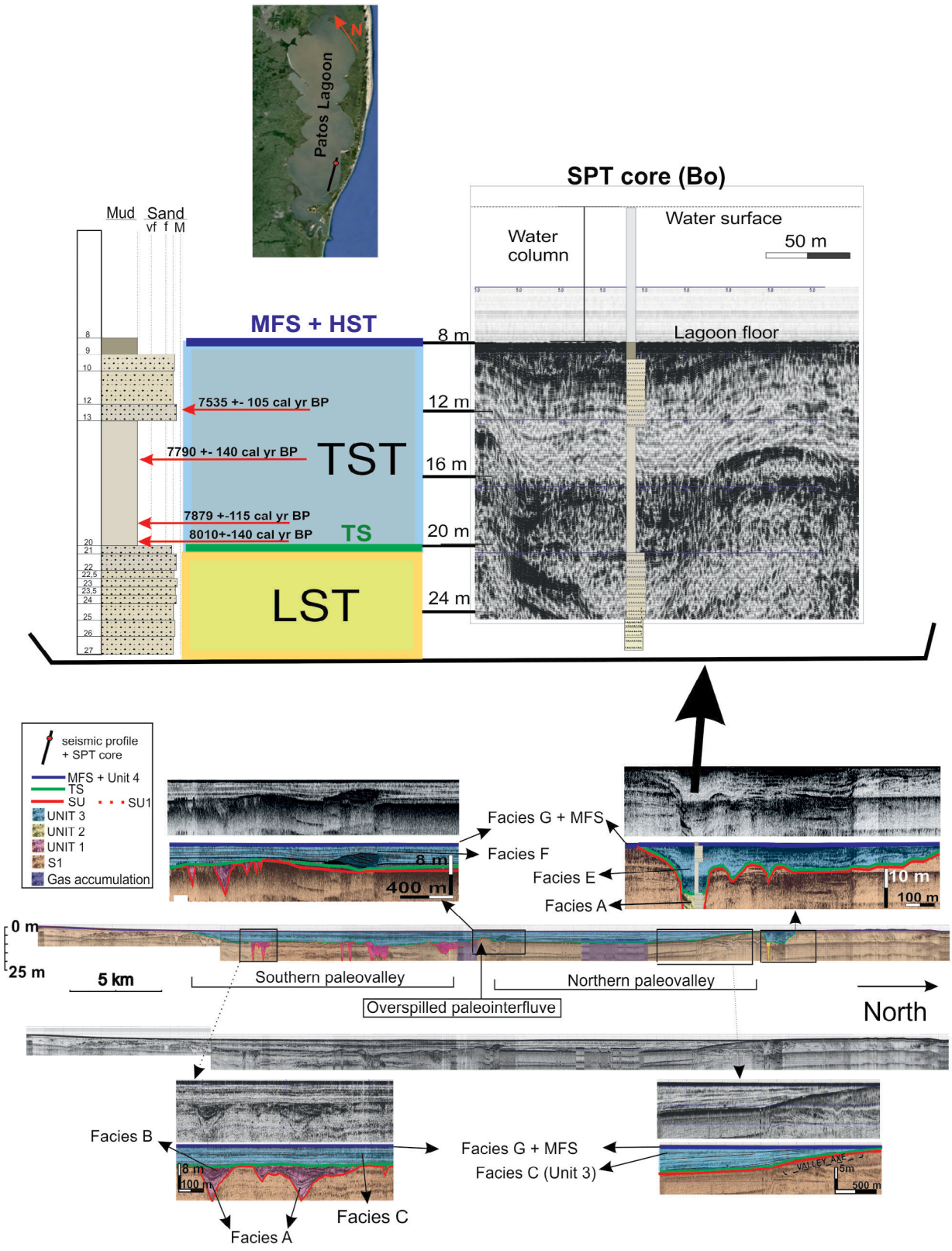

Figure 3. Seismic line 2 with the seismic facies identified, tied to Bo core and system tracts individualization (Bo core and seismic line 2 are modified from Weschenfelder *et al.* 2014). Radiocarbon dating from (Baitelli 2012, Weschenfelder *et al.* 2014, Santos-Fischer *et al.* 2016).

to be inclined when onlaping the valley's axes, where they form a wedge shape. Some reflectors of Facies C show high amplitude and trap the gas accumulated in older deposits (Weschenfelder *et al.* 2006, 2016). Such trapping layers are interpreted as stiff muddy sediments and are mappable for long distances. The SPT cores Mo and Pa (Figs. 3 and 5) and gravity cores PT-05 and PT-01 described in Bortolin *et al.* (2018) reached this facies, revealing a succession of muddy layers. These deposits are interpreted as estuarine sediments or sediments of evolving lagoons.

Facies D (Figs. 2 and 5) is a package in a mounded geometry, reaching more than 15 m thick, comprising bidirectional and progradational reflectors. It is covered in a toplap by the Maximum Flooding Surface (MFS), that touches the contemporary bathymetry. An alternation between high and low amplitude reflectors is corroborated with core PT-08 (Fig. 5), reflecting intercalated sandy and muddy layers, that resisted gravity core penetration. Northward, the reflectors are more continuous and less inclined in comparison with the southward portion of the mound form (Fig. 5). The age of 4,747 ± 98 cal yr BP was determined for these deposits by radiocarbon dating carried out in sample shells at 0.60 m depth; the shell species could not be identified due to physical weathering (Bortolin *et al.* 2018). This is interpreted as a bayhead delta.

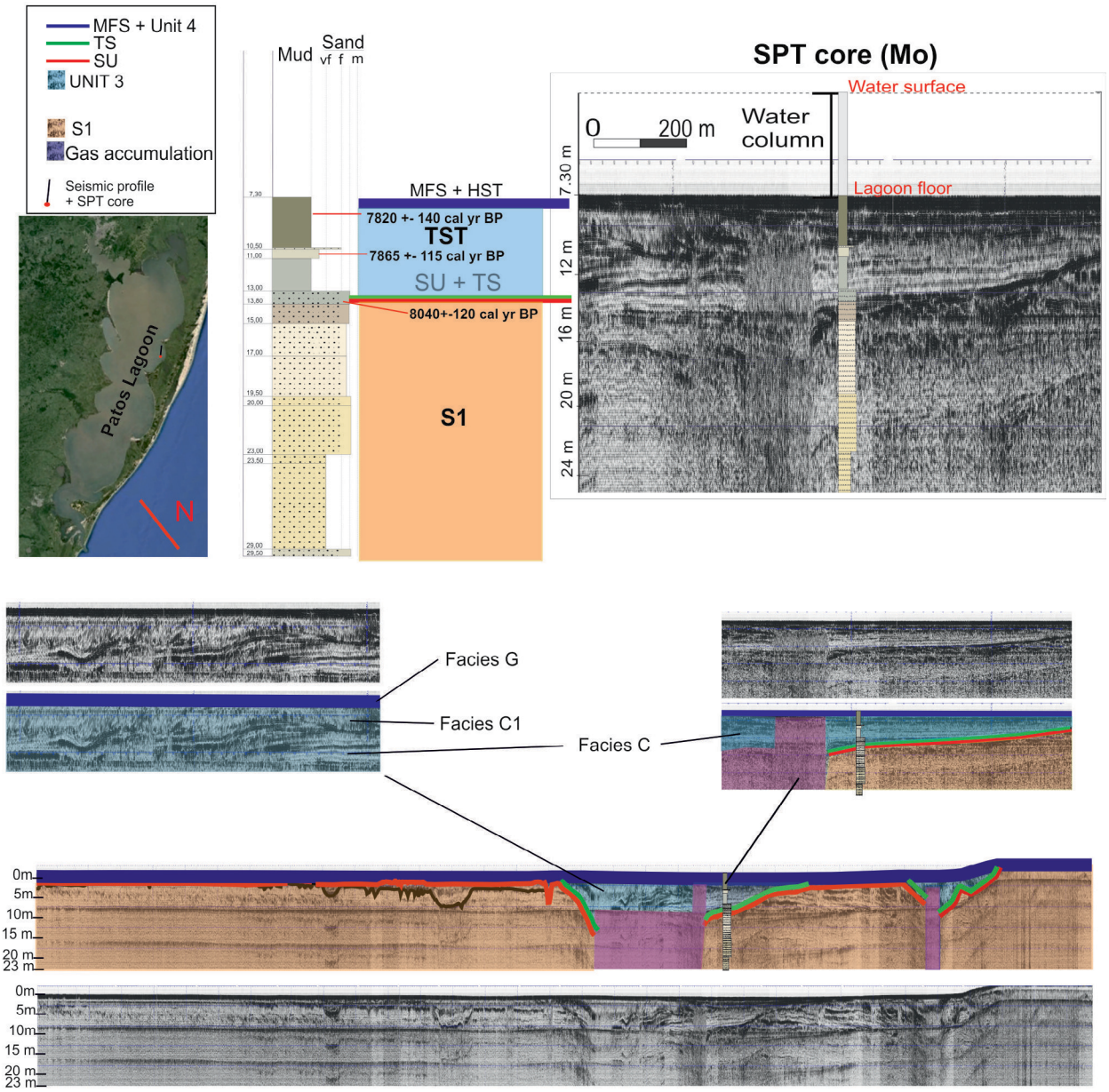

Figure 4. Seismic line 7 with the seismic facies identified, tied to Mo core and system tracts individualization (Mo core and seismic line 7 are modified from Weschenfelder *et al.* 2014). Radiocarbon dating from (Baitelli 2012, Weschenfelder *et al.* 2014, Santos-Fischer *et al.* 2016).

Facies E (Figs. 2 and 3) occurs within the remaining inlet channels and presents reflectors with a mixed aggradational/progradational pattern, variable amplitude, parallel to sub parallel, wavy, filling channel geometry, high frequency and variable continuity. In the upper portion, some scour created by reactivation of the channels are present. Small variations in these parameters made Weschenfelder *et al.* (2005, 2008b) individualize this package in many sub-facies (in the Bojuru channel, seismic line 2). The current study grouped those sub-facies into Facies E, because for environmental evolution analysis they have the same meaning. This facies is also described by Weschenfeder *et al.* (2010a) in paleochannels of seismic lines 2 and 7, reporting it as presenting multiple wavy reflectors, continuous to discontinuous, with variable amplitude, whose uppermost portion is truncated by modern reflectors (scouring), and is interpreted as channel infilling by estuarine and marine transgressive clays. Fossil assemblages identified in these deposits present a high marine influence (Santos-Fischer *et al.* 2016, Dehnhardt 2017) and are revisited in the discussion. This facies is interpreted as an inlet fill.

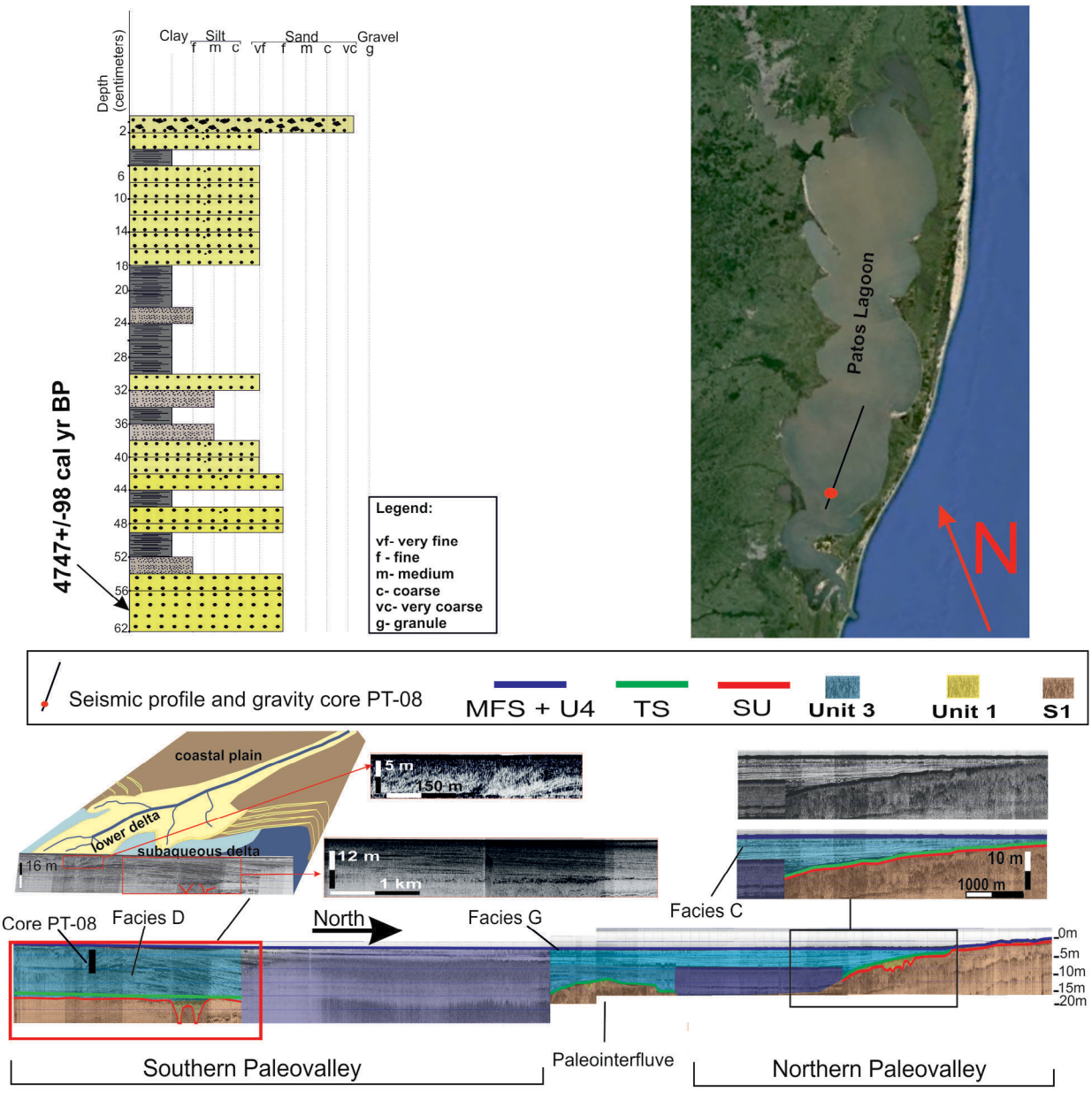

Figure 5. Seismic line 12 with the seismic facies identified, tied to PT-08 core and system tracts individualization. On average, 6 m of water column is recorded over the lagoon floor. PT-08 core and radiocarbon dating are from Bortolin *et al.* (2018).

Facies F (Figs. 2 and 3) is a progradational/aggradational package. It is typified by reflectors with high amplitude, low frequency, medium continuity, oblique and with the external geometry in bank. Facies F occurs next to a paleotopographic high, which is onlapped (from southwest to northeast) until over-spilling occurred, forming a bank geometry on the northeast side. Layers of Facies C conformably overlie the bank, indicating that Facies F was formed during an earlier stage of Holocene sea-level rise. This facies is interpreted as a sandy bank, generated by the sands eroded during the overspilling of a topographic high, which comprises pre-LGM substrate.

Facies G (Figs. 2 to 6) represents the thin layer (0.5 m) of modern sediments, deposited since the interfluves were flooded and the current back-barrier lagoon was established. This facies is the single one of Unit 4, whose lower limit is the MFS and the upper limit is the lagoon floor. It is characterized by high amplitude reflectors, with lateral continuity, capping all the previous deposits. The cores Bo, Mo and Pa show it as a muddy layer on the top of the sequence.

Seismic units

The sequences (S1, S2 and S3) were defined by Weschenfelder *et al.* (2014), separated by unconformity surfaces (SU and SU1). In the current work, seismic units will be organized within these sequences, correlated to a specific system tract, following the stratigraphic concepts proposed by Catuneanu *et al.* (2011). The seismic facies, identified in each seismic unit, will be interpreted as a specific depositional environment (Figs. 2 to 6).

Unit 1

Grouped in Unit 1 are the early fluvial channel facies (A and B) and early estuarine facies (C). The Unit 1 is underlain by the SU surface, capped by the SU1 surface and is interpreted as the Falling-Stage System Tract (FSST). These deposits have a channel infilling geometry, with concentric infilling reflectors, that become increasingly horizontal upwards as the channel is infilled. Radiocarbon dating revealed ages older than 43 ky BP; all three dated samples (Tab. 1) in U1 were of *Nucula semiornata* (Baitelli 2012, Weschenfelder *et al.* 2014).

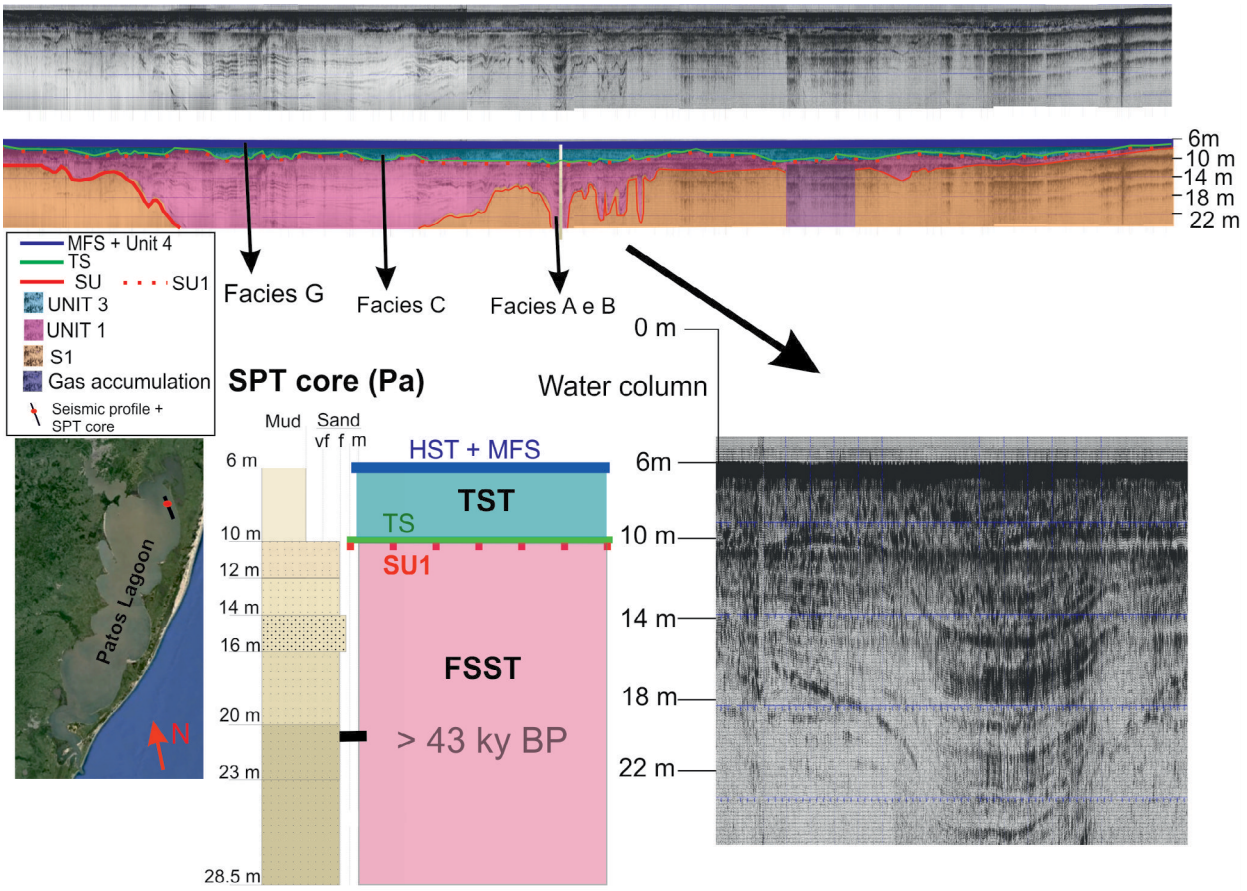

Figure 6. Seismic line 22 with the identified seismic facies, tied to Pa core and system tracts individualization. Pa core and seismic line 22 are modified from Weschenfelder *et al.* (2014). Radiocarbon dating from (Baitelli 2012, Weschenfelder *et al.* 2014).

On the top of U1 an unconformity surface can be identified (SU1). This surface is represented by a high-amplitude, irregular reflector with several small channels (< 2 m depth) (Fig. 6). This surface was probably developed during successive subaerial exposures of this coastal area along the FSST.

Unit 2

This unit is the record of the fluvial channel facies (facies A and B) formed during the LGM (Figs. 2 and 3). Such channels reached the lowest depths recognized in the Upper Sequence (> 25 m), in agreement with the lowest sea level position, around 120 m lower than the current level. It was reached by only one core (Fig. 3). The samples collected are fine to medium sands, with shell fragments.

These deposits have channel infilling geometry, with concentric infilling reflectors, increasing horizontality of strata upward as the channel is infilled. The stratification patterns (internal configuration of reflectors) of this unit show the same characteristics as the fluvial facies of Unit 1, hence they are interpreted as the same seismic facies (A and B). However, despite having the same physical characteristics, they are in distinct stratigraphic positions and therefore represent different system tracts. Unit 2 deposits are over an unconformity surface and under the transgressive surface (TS).

Weschenfelder *et al*. (2005, 2006, 2016) recognized a close spatial association between gas concentrations in central portions of the lagoon with paleotopographic depressions, which could be caused by fluvial incisions and were infilled by transgressive sediments. The gas concentrations are linked to Units 1 and 2 and provide clues to these units' identification.

Unit 3

U3 exhibits mainly aggradational reflectors, secondarily progradational or mixed pattern, grouping estuarine (C), bayhead delta (D), inlet (E) and overspilling (F) facies. The base of U3 is marked by the TS, and the top is delimited by the MFS surface (both surfaces described ahead). U3 therefore comprises the Transgressive System Tract (TST). The cross sectional geometry of this unit is typical of U-shaped valley infilling (Gibling 2006) (Fig. 3), which has high width/depth ratios and increasing width oceanward. The valley widths are 35 km on average; the depths are variable, peculiar to each lagoon morphologic cell, but usually around 30 m.

Radiocarbon dating revealed Holocene ages (Baitelli 2012, Santos-Fischer *et al*. 2016, Weschenfelder *et al*. 2014) for these deposits (Figs. 3, 4 and 5). The shell species sampled for radiocarbon dating in Mo core were *Erodona Mactroides* (8 m depth), *Clausinella gayi* (11 m depth), *Clausinella gayi* (13 m depth); for Bo core were *Ostrea equestris* (12 m depth), *Heleobia australis* (15 m depth), *Heleobia australis* (19 m depth) and shell fragments (20 m depth). The samples are organized in Table 1.

Unit 4

Unit 4 caps all the previous deposits and is recognized in all seismic lines. Its basal limit is the MFS and the top is limited by the lagoon floor. One single facies (G) composes this unit; it has an average thickness of 50 cm, hampering the visualization in the figures, therefore the MFS and Unit 4 are represented together. Facies G represents the deposits accumulated since all the interfluves were flooded and the current back-barrier lagoon was formed.

Discontinuity surfaces

The discontinuity surfaces represent a switch in stratification pattern (a reflector's internal configuration), beyond which a new group of facies with distinct patterns of reflectors occurs. They are generated by contrasts in acoustic impedance or changes in the geometric relationship between the strata, which are perceivable regionally and allow the identification of seismic units.

The subaerial unconformity (SU) underlines the depositional sequence S2. It is evidenced seismically by an irregular reflector, of high amplitude, continuous for tens of kilometers, underlying the incised valleys. It is marked by the truncation of older reflectors and its upper limit is characterized by the onlap/downlap of aggrading flooding reflectors.

The SU1 is represented by a high amplitude, irregular reflector, continuous for tens of kilometers which occur on the top of Sequence 2 deposits. Small channels (< 2 m depth) can be noted on this surface (Fig. 6). SU and SU1 are juxtaposed in case of hiatus of Sequence 2 deposits, being represented together as SU.

Mo core reached the juxtaposed surfaces, SU + SU1 (Fig. 4). The sedimentary sample collected (13.8 to 15 m depth) evidences this composite surface as a stiff sandy substrate, iron-oxide-rich, likely formed under subaerial conditions, such as pedogenesis and fluvial process. The deepest SU segments are located at the central portions of the valleys, more specifically at the substrate of the fluvial channels. On the other hand, the shallowest portions are located on valley interfluves and are thinly covered by sediment.

TS marks the transition from the early infilling facies, to the post-LGM transgressive facies. It is recorded as a high amplitude and continuous reflector, conformably overlying the earlier deposits or the subaerial unconformity surfaces. It appears juxtaposing the SU/SU1 segments where the fluvial facies are not present.

MFS is distinguished by a continuous, high-amplitude reflector, conformably overlying the earlier deposits, and

is located about 50 cm depth. It represents the complete drowning of the interfluvial areas and the establishment of the modern geomorphological pattern of the modern Patos Lagoon.

DISCUSSION

Like other lagoons with non-migrating barriers (Benallack *et al.* 2016), the Patos Lagoon favors the preservation of Late Pleistocene/Holocene geologic records, because the stable sandy coastal barriers minimize transgressive ravinement by ocean waves and tides. The microtidal range likewise limits tidal ravinement. Moreover, the majority of the deposits in the lagoon are transgressive mud, allowing satisfactory acoustic signal penetration and facilitating gravity coring.

Paleodrainage systems were active on the RS coastal plain during pre-Holocene falling and lowstand stages, which exposed the Rio Grande do Sul continental shelf, when sea level was 120/130 m lower than the present level (Corrêa 1986, Weschenfelder *et al.* 2005, 2010a, 2010b, 2014, Baitelli 2012, Bortolin 2017, Bortolin *et al.* 2018). These moments are recorded in our data by discontinuity surfaces in the sedimentary sequence, SU and SU1.

Seismo-stratigraphic characteristics including irregularity of reflectors, high amplitude, continuity for tens of kilometers, truncation of older strata, iron-oxide-rich stiff sandy layer (attested by Mo core), as well as their position underlying incised valleys suggest SU and SU1 as subaerial unconformities, marking the period when the shelf was exposed (Corrêa 1986, Angulo *et al.* 2006, Nordfjord *et al.* 2006, Baitelli 2012, Weschenfelder *et al.* 2014, Bortolin 2017, Bortolin *et al.* 2018). These surfaces can be interpreted as regional unconformities, because of their continuity through the adjacent morphologic cells of Patos Lagoon (Figs. 3, 4, 5 and 6). They were generated during the Pleistocene glaciations, eroding previous deposits (S1), which were formed during the Last Full Interglacial (LFI) (Fig. 7), MIS 5e (Imbrie *et al.* 1984, Weschenfelder *et al.* 2005, 2010a, 2014, Baitelli 2012, Bortolin 2017).

Sequence 1 is represented by reflectors with high parallelism, good lateral continuity and variable amplitude. These previous deposits (S1) probably were generated during a period of high sea level, likely are cohesive mud or cemented sandy barriers from paralic environments. This substrate can be very resistant to erosion, also can inhibit the lateral migration of early fluvial channels, generating the V-shaped channels (facies A and B), which were incised and infilled by vertical adjusts (Fielding *et al.* 2005; Gibling 2006).

Other researchers have also recognized differences in the architectural strata between initial phases of excavation (or early infilling) and late infilling of fluvial channels (*e.g.*, Fielding *et al.* 2005). The early infilling phase (Facies A, Fig. 2) is represented by confined channel infilling, with reflectors of low amplitude, which are symmetrical and concentric. The final infilling (Facies B) is characterized

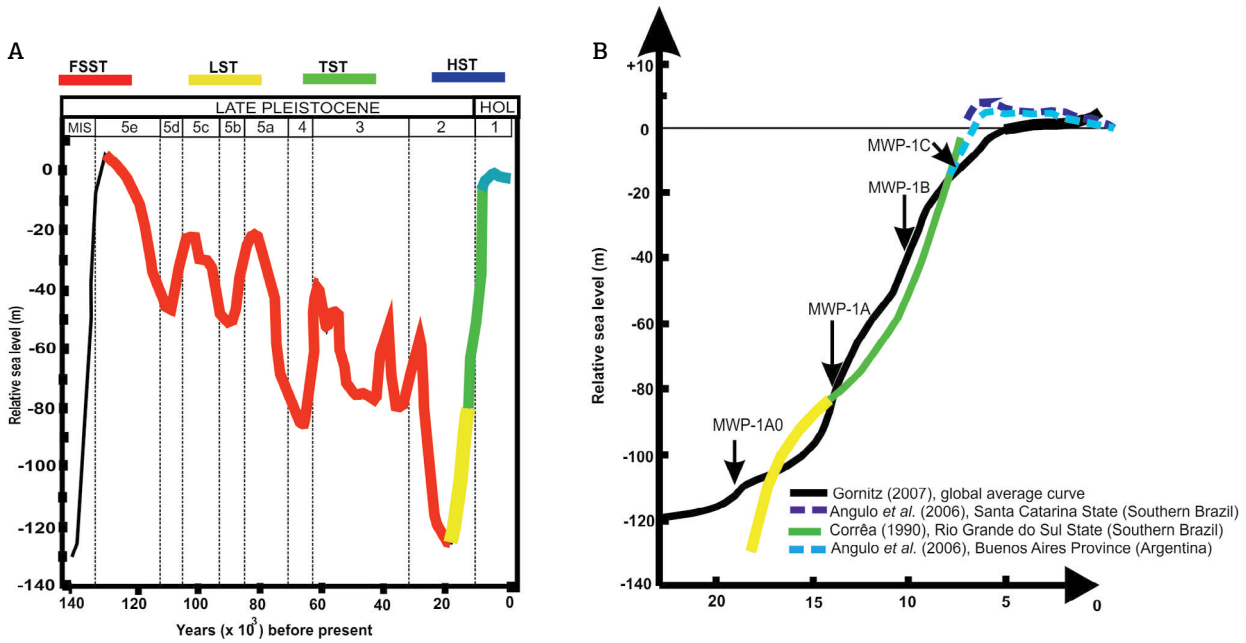

Figure 7. (A) Tentative of correlation between late Pleistocene high-frequency sea level changes and identified system tracts. Sea level curve based on Imbrie *et al.* (1984) Marine Isotope Stages; (B) detailed sea level curve for the area and surroundings, since Last Glacial Maximum (LGM), properly referenced in the figure.

by variable reflectors amplitude; some strong reflectors are common, and increase in horizontality of the layers upward. The amplitude homogeneity in reflectors of Facies A probably represents an infilling by homogeneous sediment, while the variable reflectors of Facies B might reflect alternation between muddy and sandy sediments. This organized infilling architecture recognized in fluvial paleochannels contrasts with seismo-stratigraphic classical models (Nordfjord *et al.* 2006, Green *et al.* 2013) and are similar to the descriptions of Fielding *et al.* (2005) and Gibling (2006).

The rivers lose transport competence during subtle relative sea level rises or stillstands that occurred since MIS 5e (Fig. 7A), adjusting their equilibrium profile by depositing bedload. Rivers unable to migrate laterally have to adjust their equilibrium profile vertically, aggrading symmetric and concentric bedload layers, forming facies A and B, which are recognized within the FSST and Lowstand System Tract (LST). The notable differences in basal and upper fluvial infilling (facies A and B) is associated to the adjustment of the river to changes in base level (Fielding *et al.* 2005, Gibling 2006).

Gas concentrations were recognized in central portions of Patos Lagoon, where paleotopographic depressions were infilled by transgressive fine sediments (Weschenfelder *et al.* 2005, 2006, 2016). These paleodepressions could be generated or occupied by fluvial channels along regressive events and infilled during the subsequent transgressive event (Weschenfelder *et al.* 2005, 2006, 2016). Therefore, the gas records can help the mapping of the facies of Units 1 and 2 of the FSST and LST described ahead.

Falling-Stage System Tract

Classic studies based on Fisk (1944) applied the concepts of "forced regression" or "falling-stage systems tracts" as periods of incision with sediment bypass through the valley, associating the valley infilling with the lowstand and subsequent sea level rising (Posamentier & Vail 1988, Van Wagoner *et al.* 1990, Dalrymple *et al.* 1992, 1994, Posamentier *et al.* 1992, Zaitlin *et al.* 1994, Nordfjord *et al.* 2006, Green 2009, Green *et al.* 2013). The *Falling-Stage System Tract* term was applied by Catuneanu *et al.* (2011) in reference to deposits accumulated after the onset of sea level fall, and, before the start of the next relative sea-level rise, this work was a nomenclature review about sequence stratigraphy.

Modern researchers have been contesting the classic incised valley models, especially the issues approaching incision and complete sediment bypass; several studies were discussed by Blum & Törnqvist (2000) and Blum *et al.* (2013). According to these researchers, simple incision cannot create a valley-scale feature; rather it is the superposition of surface dynamics that drives the widening of an initial channel. These researchers contend that channel-belt construction and valley widening also increase the sediment input to the river mouth. However, these works affirm that while all rivers act as a bypass system to some degree, a significant percentage is trapped in the alluvial-deltaic clinothem during sea level fall. Finally, Blum *et al.* (2013) state that sediment bypass and fluvial deposition are not mutually exclusive and both processes occur during the sea level falling stage.

In the records presented in the current work, this system tract groups the deposits accumulated since the onset of sea level fall, occurred immediately after the LFI (MIS 5e), until the LGM. Unit 1 is representative of this system tract, limited by the unconformity surfaces SU and SU1; the stratigraphic position between two unconformity surfaces suggests the successive exposure expected for this system tract. Facies A, B and C were recognized in this phase. Weschenfelder *et al.* (2014) associated these deposits with the period between 120–18 ky BP and named them S2.

The seismic records classified in this work as FSST have an external geometry of channel infilling type, reflectors with variable amplitude, good lateral continuity, tending to increased horizontality upward, onlapping the margins of the valleys and channels. Samples collected in Pa core (> 10 m depth) revealed these deposits as sandy sediments (Fig. 6), older than 43 ky cal BP (Weschenfelder *et al.* 2014).

Diatom assemblages analyzed by Santos-Fischer *et al.* (2016) suggest the depositional paleoenvironment as marine-dominated with rare and uncommon freshwater, corroborating with the environment of *N. semiornata* species (Dehnhardt 2017), whose shells were used for radiocarbon dating of these deposits (Tab. 1). These fossils also provide information about the adjacent environment, which is important in such dynamic coastal zones. The Late Pleistocene sea level fall was not constant and had minor rises in sea level during the process (Imbrie *et al.* 1984). The marine dominance reported by Santos-Fischer *et al.* (2016) suggests the sea as an adjacent environment extremely influential on coastal drainage systems, which had their incised valleys partially infilled by alluvial facies.

Paleochannels excavated the S1 during the early process of sea level fall, after MIS 5e (Fig. 7). Subsequently, gentle sea level rises (Fig. 7) probably forced the rivers to accumulate bedload in their channels, facies A and B of Unit 1. In topographically lower areas, the increase in water level formed early estuarine deposits, Facies C of U1.

FSST deposits were formed during the early stages of sea level fall; probably they were subaerially exposed several times, mainly during LGM. A hiatus of deposition is recorded on the top of these deposits, because the LST deposits were not recorded over FSST, maybe because the river migrated to a new drainage line (Baitelli 2012, Weschenfelder *et al.*

2014, Bortolin 2017, Bortolin *et al.* 2018). This suggests that the FSST sediments were completely flooded again during the Holocene sea level rising, when they were covered by the TST deposits (Figs. 2 and 3).

Lowstand System Tract

According to Catuneanu *et al.* (2011), the LST deposits accumulated after the onset of relative sea level rise, on the top of the FSST and the corresponding subaerial unconformity. In our records, the LST includes the package of deposits accumulated after the LGM (Fig. 7), during the onset of the post-glacial sea level rise. Unit 2 is representative of this system tract and is composed of facies A and B.

The LST deposits presented in our records appear directly over the SU + SU1 composite surface, where FSST were either eroded or not deposited (Fig. 3). The seismo-stratigraphic signature of these deposits is characterized by sandy packages, with reflectors organized with a channel infilling geometry, representing a symmetric and concentric infilling (Fielding *et al.* 2005, Gibling 2006). Earlier studies based on seismic line 2, interpreted basal deposits in the channel of Bojuru region (Fig. 1) as fluvially generated (Weschenfelder *et al.* 2005, 2008b, 2010a), in agreement with the results presented in this study.

Classic studies of fluvial sediments accumulating over unconformity surfaces describe these deposits with a chaotic internal configuration of reflectors (Nordfjord *et al.* 2006, Green 2009, Green *et al.* 2013). In contrast, our records represent fluvial facies with moderate architectural organization in the form of concentric infilling and moderate symmetry, similar to examples reported by Fielding *et al.* (2005) and Gibling (2006).

According to Corrêa (1986), sea level was at -120/130 m during the LGM, the lowest level in the analyzed period (since MIS 5e, Fig. 7). During the LGM, the Camaquã and Jacuí rivers would have promoted scouring of new routes, around the Bojuru region for the Camaquã River and Mostardas for the Jacuí River (Weschenfelder *et al.* 2010b, 2014, Baitelli 2012). This reorganization of drainage lines to adjacent areas can be explained by differences created in paleotopography as a consequence of sediment input (Bortolin 2017). These rivers partially infilled the valleys occupied by them during FSST, then switched their waterways to lower unfilled areas due an increase in potential energy, which was generated by the lowest base level (LGM). This model is discussed in Bortolin (2017), and similar models are presented in Bishop (1995) and Brocard *et al.* (2011).

The influence of the adjacent marine environment on these alluvial systems is recorded by diatom assemblages, analyzed by Santos-Fischer *et al.* (2016), that record the partial flooding of these channels. This can be expected during the onset of sea level rising which characterizes the LST (Catunenanu *et al.* 2011).

Transgressive System Tract

According to Catuneanu *et al.* (2011), TST includes deposits that accumulated from the onset of transgression until the time of maximum transgression of the coast. The current work interprets the TS surface as a marker of the beginning of the TST, over which a succession of retrogradational/transgressive layers accumulated. The Holocene flooding increased accommodation space vertically and laterally, with stepwise onlap of interfluves (Bortolin 2017, Bortolin *et al.* 2018). The TST comprises the deposits of Unit 3, which are overlain by the MFS and includes facies C, D, E and F.

TS is recorded in the seismic data as a high amplitude and continuous reflector, conformably overlying the earlier alluvial facies or the subaerial unconformity, and the underlying estuarine deposits. It appears juxtaposed with the SU segments where the fluvial facies are not present (valley margins). When the fluvial facies are present, the TS blankets facies B deposits, which represent the upper infilling part of the fluvial channels, indicating progressive flooding. A similar Holocene blanket was described in fluvial systems from northern-eastern Australian rivers (Fielding *et al.* 2005).

Different velocities of sea level rise were reported by Corrêa (1986) during the post-LGM transgression on the Rio Grande do Sul shelf. Marine terraces were developed during stabilizations of sea level, which were then submerged during accelerated sea level rise (2 cm/year). The rates of muddy estuarine deposition were very high in some packages of the TST, reaching 1.8 cm/year (8,040 ± 120 cal yr BP to 7,820 ± 140 cal yr BP) at some locations (Bortolin 2017, Bortolin *et al.* 2018). This may be associated with periods of rapid sea level rise (Melt Water Pulses — MWP; Gornitz 2007, Smith *et al.* 2011, Bortolin 2017, Bortolin *et al.* 2018, Santos-Fischer *et al.* 2018) and are recorded by C-14 dating (Figs. 2 and 3).

Facies C in the TST represents a homogeneous succession of muddy layers, recorded by Mo, Pa and gravity cores (Bortolin *et al.* 2018). The strata have external sheet form, good horizontality, high continuity (kilometer scale), high frequency and well-formed parallelism among the layers. The layers tend to be horizontal in the central portion and inclined where they onlap the valley margins. The sediment did not offer strong resistance to gravity coring, and its geotechnical characteristic indicates that it is not consolidated. These muddy layers have low porosity and serve to trap gas migrating from older deposits (Weschenfelder *et al.* 2006, 2016). This transgressive muddy package was deposited in a low energy environment, filling up the incised valley

depressions. These deposits are interpreted as estuarine or from evolving lagoons.

Facies D represents a succession of layers deposited in an environment with variable energy, attested by PT-08 core, which shows alternation between clays, silts, sands and gravel (Bortolin *et al.* 2018). This facies is interpreted as a bayhead delta, because of the external geometry of the facies in mound form, the internal configuration with bidirectional progradational clinoforms and alternation between coarse and thin sediments, indicating pulses of increased river discharge.

Bayhead deltas are common in the landward portion of wave dominated estuaries (Dalrymple *et al.* 1992, Zaitlin *et al.* 1994). The most probable streams to develop this deposit are the Contagem, Corrientes and Turuçu, south of the Camaquã River (Manzolli 2016). Based on radiocarbon dating, the topmost unit (last 0.60 m) was deposited around 4,747 ± 98 cal yr BP.

It appears that deposition of these deltaic facies ceased during the end of the TST and beginning of highstand system tract (HST), around 5 ky BP on the RS coastal plain (Fig. 7) (Corrêa 1986, Angulo *et al.* 2006). Another possibility is that these deposits (Facies D) are older deltaic records, reworked by transgressive estuarine processes, mixing the deltaic deposits with the modern transgressive infilling, including shells. The shell collected for radiocarbon dating was on the top of the deltaic package (0.60 m depth), which is the most vulnerable portion for sediment reworking in an energetic and dynamic environment. The shell was poorly preserved, and the species was not recognizable.

Facies E is interpreted as an infilled tidal inlet, because of the external geometry in channel fill type, wavy reflectors (suggesting a wave-influenced environment), which are organized in an aggradational/progradational stratification pattern with recurrent erosional scouring in the upper portion. Similar scouring in the upper portion of channel infill was interpreted by Green *et al.* (2013) as suggestive of local scale tidal scouring within an inlet complex. Studies carried out on seismic line 2, interpreted fluvial facies on the basis of this facies (Weschenfelder *et al.* 2005, 2008b, 2010a), corroborating the results presented in this study. Fluvial channel negative relief can remain active as inlets during transgressions, particularly in the most prominent incisions (FitzGerald *et al.* 2012, Bortolin *et al.* 2018). Probably, the paleocourses of the Jacuí and Camaquã rivers occupied during the LGM remained active as Holocene inlets (Weschenfelder *et al.* 2010b, 2014, Bortolin 2017, Bortolin *et al.* 2018).

Alternatively, to the model presented in these work, earlier fluvial deposits might be removed during marine ingressions by inlets, which could explain the marine influence recorded by fossil samples (Weschenfelder *et al.* 2008b, Santos-Fischer *et al.* 2016).

Palynomorph, diatom and seismo-stratigraphic evidence allowed the interpretation of Facies E as an inlet, because of the mixed influence of marine and freshwater paleofossils (Weschenfelder *et al.* 2008b). Santos-Fischer *et al.* (2016) analyzed diatom assemblages, selected from samples of the SPT boreholes performed in paleochannel locations, concluding that these facies were strongly influenced by marine conditions during the Holocene.

The diatom assemblages analyzed by Santos-Fischer *et al.* (2016) represent the proximity between these channels and the sea, and also suggest high segmentation of the Holocene coastal barrier. The high accumulation rates reported in these channels for mid-Holocene (Bortolin 2017, Bortolin *et al.* 2018) represent the drowning of these systems, caused by a marine ingression, attested by the predominantly marine diatom assemblages (Santos-Fischer *et al.* 2016). This sedimentary drowning occurred relatively fast at rates of 1.8 cm/year (8,040 ± 120 cal yr BP to 7,820 ± 140 cal yr BP), possibly as a consequence of the 8.2 ky BP Melt Water Pulse event (Gornitz 2007, 2012, Smith *et al.* 2011, Bortolin 2017, Bortolin *et al.* 2018, Santos-Fischer *et al.* 2018).

The Holocene coastal barrier was developing ~ 2 km seaward of its present position during the late Holocene in the Bojuru region, creating an interbarrier paleolagoon, between Pleistocene and Holocene coastal barriers (Dillenburg *et al.* 2004). In this area, Facies E is likely related to a former connection between the Patos Lagoon, the interbarrier lagoon and the ocean. Similar examples of interbarrier lagoons currently connected to each other and with the ocean are also present in South Africa (Cawthra *et al.* 2014, Benallack *et al.* 2016).

Coastal ponds or marshy swales can be indicative of relict inlets (FitzGerald *et al.* 2012); such situation is found at the Barra Falsa feature in the Bojuru locality (Toldo Jr. *et al.* 1991, Weschenfelder *et al.* 2014). Besides Barra Falsa, other low relief morphologic features were recognized in eastern Patos Lagoon margins, such as the lakes Rincão, Reserva and Gateados (Fig. 1). These features are directly in front of the paleochannels recognized by seismic interpretations in Patos Lagoon and also could be indicative of former Holocene inlets (Bortolin 2017, Bortolin *et al.* 2018).

Facies F is interpreted as sedimentation resulting from overspilling of a paleointerfluve (Fig. 3). The paleointerfluves in the Patos Lagoon sub bottom are illustrated by modern works analyzing the paleotopography in the region (Bortolin 2017, Bortolin *et al.* 2018). The major factor controlling the overspilling was sea level rise, which caused the flooding of isolated estuarine areas, whose interfluves subsequently suffered overspilling, unifying the evolving estuaries (Bortolin *et al.* 2018). Similar overspilling was reported by

Green *et al*. (2013). The aggrading reflectors (U3) onlapping both sides of the paleointerfluve (Fig. 3) represent the sea level rising (TST) with a considerable sediment input. This model of sea level rise with positive sediment input contrasts with the case reported by Cooper *et al*. (2012) in Kosi Lagoon (South Africa), where fluvial input was negligible during transgression and the reworking of the estuarine margins caused the infilling of some deep sections of the incised valleys by slumped material.

Wind action may have exerted a secondary control in the overspilling process, during episodic events (storms). The direction of the overspilling sedimentation (from SW to NE) is consistent with winter wind directions, when the strongest storms are expected from the SW (Toldo Jr. *et al*. 2006a). Northeast winds are predominant in the region during the major part of the year, but the southwest winds are marked by the most intense storms during the winter, as frontal systems become frequent (Möller *et al*. 2001). Two paleodepressions were joined after the overspilling of the gentle interfluve (Fig. 3), forming a remarkable reflector of high continuity and moderate amplitude. This represents the rapid flooding of a large area, elucidating how single events can change dramatically the physiography of an area. It may be another example of the effects of the 8.2 ky BP MWP event.

Highstand System Tract

HST deposits are progradational deposits, developed when sediment accumulation rates exceed the rate of increase in accommodation during the late stages of sea-level rise. These sediments are deposited directly on the MFS (Catuneanu *et al*. 2011). Unit 4 blankets all previous deposits with a thin muddy layer.

MFS marks the onset of the HST deposits, which are classified in the present work as Unit 4. These deposits started to accumulate after the flooding of the interfluves unified the adjacent incised valley systems (U3) and created a large back-barrier lagoon with morphology similar to the current Patos Lagoon configuration (U4). These deposits began to accumulate after the maximum sea level (+5 m), around 5 ky BP (Fig. 7), after which a gentle sea-level fall is reported for the area (Corrêa 1986, Dillenburg *et al*. 2004, Angulo *et al*. 2006), during a period of stabilization of the Holocene coastal barrier.

The sedimentation rates dropped by four orders of magnitude from U3 to U4, as a result of the vast increase in size of sedimentary basin (flooding). The differences in accumulation rates in association with the seismic unit's signature can help the individualization of TST and HST (Bortolin *et al*. 2018).

The Holocene coastal barrier stabilized since the onset of a gentle sea level fall (- 2/3 m to the present), occurred following the Holocene maximum sea level (Corrêa 1986, Dillenburg *et al*. 2004, Angulo *et al*. 2006, Lima *et al*. 2013). During this period, Unit 4 (back-barrier deposits) accumulated in conditions of low energy, low accumulation rates, while the remaining inlets were closed (Bortolin *et al*. 2018). The closure of former tidal inlets in Kosi Lagoon area (South Africa) was also associated with a fall in sea level, during the late Holocene (Cooper *et al*. 2012). In addition, freshwater input started to be more influential in the salinity of Patos Lagoon during the Late Holocene, as recorded by two freshwater taxa (*Aulacoseira veraluciae* and *Aulacoseira sp.2*) that were absent since the LGM and returned around 2.4 ky BP (Santos-Fischer *et al*. 2016). This diatom assemblage suggests the damming caused by the juxtaposition of the Holocene barrier to Pleistocene Barrier III and the associated back-barrier flooding (Bortolin *et al*. 2018).

CONCLUSION

Incised valley infilling did not occur entirely during periods of sea-level rise. It also happened during the FSST. However, during the sea-level rise the accommodation space created was more extensive.

The vertical variability of facies is attributed to sea-level oscillations, while the lateral variability is due to autogenic forcing factors.

The occurrence of a type of seismic facies is not limited to a specific system tract, but it represents the prevailing sea level trend. Facies A and B occur during sea-level fall and lowstands, when rivers drained the exposed coastal plain. Facies C was deposited during pulses of sea-level rise, when the river channels were flooded. Facies D, E and F record flooding events. Facies G was deposited after the maximum flooding was reached.

The V-shaped geometry of facies A and B was due to the stiff substrate, comprising of cohesive mud or pedoginised sandy barriers, deposited during previous highstands. The confined pattern of facies A and B restricted the lateral adjustment of rivers, which were forced to adjust their equilibrium profile by vertical accretion, accumulating bedload by loss of transport competence.

The Pleistocene drainage basins became continental depositional basins in which the main infilling deposits are transgressive muds of estuarine paleoenvironment.

The accommodation space increased both vertically and laterally with the flooding of continental areas.

The Patos Lagoon evolved and reached its current configuration after the flooding of the adjacent incised valleys.

ACKNOWLEDGMENTS

The research has been financially supported by Brazilian National Council for Scientific and Technological Development (CNPq), Formation Program in Human Resources in Geosciences (Programa de Formação de Recursos Humanos em Geociências, nº 215 — PRH-PB215), Postgraduation Program in Geosciences (Programa de Pós-Graduação em Geociências — PPGGEO) and Coastal and Marine Geology Studies Center/Federal University of Rio Grande do Sul (Centro de Estudos de Geologia Costeira e Oceânica/Universidade Federal do Rio Grande do Sul — CECO-UFRGS).

REFERENCES

Abreu J.G.N. & Calliari L.J. 2005. Paleocanais na plataforma interna do Rio Grande do Sul: Evidências de uma drenagem fluvial pretérita. *Revista Brasileira de Geofísica*, **23**(2):123-132. http://dx.doi.org/10.1590/S0102-261X2005000200002

Angulo R.J., Lessa G.C., Souza M.C. 2006. A critical review of Mid- to Late-Holocene sea-level fluctuations on the eastern Brazilian coastline. *Quaternary Science Reviews*, **25**:486-506. https://doi.org/10.1016/j.quascirev.2005.03.008

Baitelli R. 2012. *Evolução Paleogeográfica do Sistema de Paleodrenagem do Rio Jacuí na Planície Costeira do Rio Grande do Sul*. PhD Thesis, Universidade Federal do Rio Grande do Sul, Porto Alegre, 148 p. http://hdl.handle.net/10183/56850

Barboza E.G., Ayup-Zouain R.N., Tomazelli L.J., Rosa M.L.C.C., Ferreira H.P.L. 2005. Paleocanal pleistocênico na barreira III entre o Chuí e o Balneário Hermenegildo-Rio Grande do Sul. *In*: Congresso da Associação Brasileira de Estudos do Quaternário, 10., Guarapari. *Atas*... Guarapari. 1 CD.

Benallack K., Green A.N., Humphries M.S., Cooper J.A.G., Dladla N.N., Finch J.M. 2016. The stratigraphic evolution of a large back-barrier lagoon system with a non-migrating barrier. *Marine Geology*, **379**:64-77. http://dx.doi.org/10.1016/j.margeo.2016.05.001

Bishop P. 1995. Drainage rearrangement by river capture, beheading and diversion. *Progress in Physical Geography*, **19**(4):449-473. https://doi.org/10.1177%2F030913339501900402

Blum M.D. & Törnqvist T.E. 2000. Fluvial responses to climate and sea-level change: a review and look forward. *Sedimentology*, **47**:2-48. https://doi.org/10.1046/j.1365-3091.2000.00008.x

Blum M., Martin J, Milliken K., Garvin M. 2013. Paleovalley systems: Insights form Quaternary analogs and experiments. *Earth-Science Reviews*, **116**:128-169. https://doi.org/10.1016/j.earscirev.2012.09.003

Bortolin E.C. 2017. *Paleovales Quaternários na Lagoa dos Patos, Rio Grande do Sul, Brasil: preenchimento, evolução e influência na dinâmica lagunar*. PhD Thesis, Universidade Federal do Rio Grande do Sul, Porto Alegre, 113 p. http://hdl.handle.net/10183/172160

Bortolin E.C., Weschenfelder J., Cooper A. 2018. Holocene evolution of Patos Lagoon, Brazil: The role of antecedent topography. *Journal of Coastal Research*. https://doi.org/10.2112/JCOASTRES-D-17-00195

Brocard G., Teyssier C., Dunlap W.J., Authemayou C., Simon-Labric T., Cacao-Chiquín E.N., Gutiérrez-Orrego A., Morán-Ical S. 2011. Reorganization of a deeply incised drainage: role of deformation, sedimentation and groundwater flow. *Basin Research*, **23**:631-651. https://doi.org/10.1111/j.1365-2117.2011.00510.x

Catuneanu O. 2006. *Principles of sequence stratigraphy*. Amsterdam, Elsevier. 375 p.

Catuneanu O., Galloway W.E., Kendall C.G.S.t.C., Miall A.D., Posamentier H.W., Strasser A., Tucker M.E. 2011. Sequence Stratigraphy: Methodology and Nomenclature. *Newsletters on Stratigraphy*, **44**(3):173-245. https://dx.doi.org/10.1127/0078-0421/2011/0011

Cawthra H.C., Bateman M.D., Carr A.S., Compton J.S., Holmes P.J. 2014. Understanding Late Quaternary change at the land-ocean interface: a synthesis of the evolution of the Wilderness coastline, South Africa. *Quaternary Science Reviews*, **99**:210-233. https://doi.org/10.1016/j.quascirev.2014.06.029

Cooper J.A.G., Green A.N., Wright C.I. 2012. Evolution of an incised valley coastal plain estuary under low sediment supply: a "give-up" estuary. *Sedimentology*, **59**:899-916. https://doi.org/10.1111/j.1365-3091.2011.01284.x

Corrêa I.C.S. 1986. Evidence of Sea Level Fluctuation in the Rio Grande do Sul Continental Shelf, Brazil. *Quaternary of South America and Antarctic Peninsula*, **4**:237-249.

Corrêa I.C.S. (1990). *Analyse Morphostructurale et Evolution Paleogeographique de la Plata-Forme Continentale Atlantique Sud-Bresilienne (Rio Grande do Sul – Brésil)*. Doctoral dissertation, Universite de Bordeaux I, Bordeaux.

Corrêa I.C.S. 1996. Les variations du niveau de la mer durant les derniers 17.500 ans BP. L'exemple de la plateforme continentale du Rio Grande do Sul-Bresil. *Marine Geology*, **130**:163-178. https://doi.org/10.1016/0025-3227(95)00126-3

Dalrymple R.W., Boyd R., Zaitlin B.A. 1994. *Incised-Valley Systems:* origin and sedimentary sequences. Tulsa, Oklahoma, SEPM Special Publication 51, 391p.

Dalrymple R.W., Leckie D.A., Tillman R.W. 2006. *Incised valleys in time and space*. Tulsa, Oklahoma, SEPM Special Publication 85, 348 p.

Dalrymple R.W., Zaitlin B.A., Boyd R. 1992. Estuarine facies models: conceptual basis and stratigraphic implications. *Journal of Sedimentary Petrology*, **62**(6):1130-1146. https://doi.org/10.1306/D4267A69-2B26-11D7-8648000102C1865D

Dehnhardt B.A. 2017. *Evolução paleogeográfica da planície costeira média do Rio Grande do Sul: Análise de fósseis calcários e silicosos em testemunhos da lagoa dos Patos*. PhD Thesis, Universidade Federal do Rio Grande do Sul, Porto Alegre, 160 p. http://hdl.handle.net/10183/172207

Dillenburg S.R., Tomazelli L.J., Barboza E.G. 2004. Barrier evolution and placer formation at Bujuru southern Brazil. *Marine Geology*, **203**:43-56. https://doi.org/10.1016/S0025-3227(03)00330-X

Diretoria de Hidrografia e Navegação (DHN). 2014. *Tide Tables*. Brasil, Diretoria de Hidrografia e Navegação.

Emery D. & Myers K. 1996. *Sequence Stratigraphy*. New Jersey, Blackwell Science Ltd., 291 p.

Fielding C.R., Trueman J.D., Dickens G.R., Page M. 2005. Geomorphology and internal architeture of the ancestral Burdekin River across the Great Barrier Reef shelf, north-east Australia. *In*: Michael D.B., Susan B.M., Suzanne F.L. (Eds.). *Fluvial sedimentology VII*. London, UK, Wiley and Sons, Special Publications International Association of Sedimentologists, **35**:321-347.

Fisk H.N. 1944. *Geological Investigation of the Alluvial Valley of the Lower Mississippi River:* U.S. United States, Army Corps of Engineers Mississippi River Commission, 78 p.

FitzGerald D., Buynevich I., Hein C. 2012. Morphodynamics and Facies Architecture of Tidal Inlets and Tidal Deltas. *In*: Davis R.A. Jr. & Dalrymple R.W. (Eds.). *Principles of Tidal Sedimentology*. New York, Springer, chapter 12.

Gibling M.R. 2006. Width and thickness of fluvial channel bodies and valley fills in the geological. *Journal of Sedimentary Research*, **76**:731-770. https://doi.org/10.2110/jsr.2006.060

Gornitz V. 2007. *Sea level rise, after the ice melted and today*. United States, National Aeronautics and Space Administration (NASA), Goddard Space Flight Center, Sciences and Exploration Directorate, Earth Science Division. Available from: <www.giss.nasa.gov/research/briefs/gornitz_09/>. Accessed on: July 2018.

Gornitz V. 2012. *The Great Ice Meltdown and Rising Seas:* Lessons for tomorrow. National Aeronautics and Space Administration (NASA), Goddard Space Flight Center, Sciences and Exploration Directorate. Earth Science Division. Available from: <www.giss.nasa.gov/research/briefs/gornitz_10/>. Accessed on: June 2018.

Green A.N. 2009. Paleo-drainage, incised valley fills and transgressive systems tract sedimentation of the northern KwaZulu-Natal continental shelf, South Africa, SW Indian Ocean. *Marine Geology*, **263**:45-63. https://doi.org/10.1016/j.margeo.2009.03.017

Green A.N., Dladla N., Garlick LG. 2013. Spatial and temporal variations in incised valley systems from the Durban continental shelf, KwaZulu-Natal, South Africa. *Marine Geology*, **335**:148-161. https://doi.org/10.1016/j.margeo.2012.11.002

Imbrie J., Hayes J.D., Martinson G., Mcintyre A., Mix A.C., Morley J.J., Pisias N.G., Prell W.L., Shackleton N.J., Hays H., Kukla G. 1984. The Orbital Theory of Pleistocene Climate: Support from a Revised Chronology of the Marine **δ**O18 Record. *In*: Berger A., Imbrie J., Saltzman B. (Eds.). *Milankovitch and Climate Understanding the Response to Astronomical Forcing Proceedings of the NATO Advanced Research Workshop Part I*. New York, Riedel Publishing, p. 269-305.

James N.P. & Dalrymple R.W. (Eds.). 1992. *Facies Models 4*. Canada, Geological Association of Canada, 586 p.

Jones E.J.M. 1999. *Marine Geophysics*. London, Wiley and Sons, 466 p.

Kjerfve B. 1986. Comparative oceanography of coastal lagoons. *In*: Wolfe D.A. (Ed.). *Estuarine Variability*. Cambridge, Academic Press, p. 63-81. https://doi.org/10.1016/B978-0-12-761890-6.50009-5

Kjerfve B. 1994. Coastal lagoons. *In*: Kjerfve B. (Ed.). *Coastal lagoon processes*. Amsterdam, Elsevier, **60**. 576 p.

Lima L.G., Dillenburg S.R., Medeanic S., Barboza E.G., Rosa M.L.C., Tomazelli L.J., Dehnhardt B.A., Caron F. 2013. Sea-level rise and sediment budget controlling the evolution of a transgressive barrier in southern Brazil. *Journal of South American Earth Sciences*, **42**:27-38. https://doi.org/10.1016/j.jsames.2012.07.002

Manzolli R.P. 2016. *Gênese e evolução do sistema laguna-barreira da feitoria*. PhD Thesis, Universidade Federal do Rio Grande do Sul, Porto Alegre, 179 p.

Marques W.C. 2005. *Padrões de variabilidade temporal nas forçantes da circulação e seus efeitos na dinâmica da Lagoa dos Patos, Rio Grande do Sul, Brasil*. MS Dissertation, Fundação Universidade do Rio Grande, Brazil, 87 p.

Mitchum R.M, Vail P.R., Sangree J.B. 1977. Seismic stratigraphy and global changes of sea level, Part 6: Stratigraphic interpretation of seismic reflection patterns in deposicional sequences. *In*: Payton C.E. (Ed.). Seismic Stratigraphy: Application to Hydrocarbon Exploration. *AAPG Memoir.*, **26**:117-133.

Möller O.O., Castaing P., Salomon J.C., Lazure P. 2001. The influence of local and nonlocal forcing effects on the sub tidal circulation of Patos Lagoon. *Estuaries*, 24, 297-311. https://doi.org/10.2307/1352953

Nordfjord S., Goff J.A., Austin Jr. J.A., Gulick S.P.S. 2006. Seismic facies of incised-valley fills, New Jersey continental shelf: implications for erosion and preservation processes acting during latest Pleistocene-Holocene transgression. *Journal of Sedimentary Research*, **76**:1284-1303. https://doi.org/10.2110/jsr.2006.108

Posamentier H.W., Allen G.P., James D., Tesson M., 1992. Forced regressions in a sequence stratigraphic framework: concepts, examples, and exploration significance. *AAPG Bulletin*, **76**:1687-1709.

Posamentier H.W. & Vail P.R. 1988. Eustatic control on clastic deposition II - sequence and system tract models. *In*: Wilgus C.K., Hastings B.S., Kendall C.G.C., Posamentier H.W., Ross C.A., Van Wagoner J.C. (Eds.). *Sea-Level Changes:* An Integrated Approach. SEPM Special Publication, **42**:125-154.

Santos-Fischer C.B., Corrêa I.C.S., Weschenfelder J., Torgan L.C., Stone J.R. 2016. Paleoenvironmental insights into the Quaternary evolution of the Southern Brazilian coast based on fossil and modern diatom assemblages. *Palaeogeography, Palaeoclimatology, Palaeoecology*, **446**:108-124. https://doi.org/10.1016/j.palaeo.2016.01.018

Santos-Fischer C., Weschenfelder J., Corrêa I.C.S., Stone J.R., Dehnhardt B.A., Bortolin E.C. 2018. A Drowned Lagunar Channel in the Southern Brazilian Coast in Response to the 8.2-ka Event: Diatom and Seismic Stratigraphy. *Estuaries and Coasts*, **41**(6):1601-1625. https://doi.org/10.1007/s12237-018-0373-z

Schumm S.A. 1993. River response to base Level Change: Implications to sequence Stratigraphy. *The Journal of Geology*, **101**:279-294. https://doi.org/10.1086/648221

Shanley K.W. & McCabe P.J. 1994. Perspectives on the Sequence Stratigraphy of Continental Strata. *AAPPG Bulletin*, **78**(4):544-568.

Smith D.E., Harrison S., Firth C.R., Jordan J.T. 2011. The early Holocene sea level rise. *Quaternary Sciences Reviews*, **30**:1846-1860. https://doi.org/10.1016/j.quascirev.2011.04.019

Toldo Jr. E.E. 1991. Morfodinâmica da Laguna dos Patos, Rio Grande do Sul. *Pesquisas*, **18**(1):58-63. https://doi.org/10.22456/1807-9806.21362

Toldo Jr. E.E., Almeida L.E.S.B., Corrêa I.C.S., Ferreira E.R., Gruber N.L.S. 2006a. Wave prediction in Lagoa dos Patos coastline, southern Brazil. *Atlântica*, **28**(2):87-95.

Toldo Jr. E.E., Ayup-Zouain R.N., Corrêa I.C.S., Dillenburg S.R. 1991. Barra Falsa: Hipótese de um canal Holocênico de comunicação entre a Laguna dos Patos e o Oceano Atlântico. *Pesquisas*, **18**:99-103. https://doi.org/10.22456/1807-9806.21349

Toldo Jr. E.E., Dillenburg S.R., Corrêa I.C.S. & Almeida L.E.S.B. 2000. Holocene sedimentation in Lagoa dos Patos Lagoon, Rio Grande do Sul, Brazil. *Journal of Coastal Research*, **16**(3):816-822.

Toldo Jr. E.E., Dillenburg S.R., Corrêa I.C.S., Almeida L.E.S.B., Weschenfelder J., Gruber N.L.S. 2006b. Sedimentação de longo e curto período na Lagoa dos Patos, Sul do Brasil. *Pesquisas em Geociências*, **33**(2):79-86. https://doi.org/10.22456/1807-9806.19516

Tomazelli J.L. & Villwock J.A. 2000. O Cenozóico no Rio Grande do Sul: Geologia da Planície Costeira. *In*: Holz M. & De Ros L.F. (Eds.), *Geologia do Rio Grande do Sul*. Porto Alegre, CICO/UFRGS, 375-405.

Van Wagoner J.C., Mitchum R.M., Campion K.M., Rahmanian V.D. 1990. *Siliciclastic sequence stratigraphy in well logs, cores, and outcrops: concepts for high-resolution correlation of time and facies*. Tulsa, AAPG Methods in Exploration, **7**:55.

Villwock J.A., Tomazelli L.J., Loss E.L., Dehnhardt E.A., Horn Filho N.O., Bachi F.A., Dehnhardt B.A. 1986. Geology of the Rio Grande do Sul Coastal Province. *In*: Rabassa J. (Ed.). *Quaternary of South America and Antarctic Peninsula*. Rotterdam, CRC Press, **4**:79-97.

Weschenfelder J., Baitelli R., Corrêa I.C.S., Bortolin E.C., Santos-Fischer C.B. 2014. Quaternary incised valleys in the southern Brazil coastal zone. *Journal of South American Earth Science*, **55**:83-93. http://dx.doi.org/10.1016/j.jsames.2014.07.004

Weschenfelder J., Corrêa I.C.S., Aliotta S. 2005. Elementos arquiteturais do substrato da Lagoa dos Patos Revelados por sísmica de alta resolução. *Pesquisas em Geociências*, **32**(2):57-67.

Weschenfelder J., Corrêa I.C.S., Aliotta S., Baitelli R. 2010a. Paleochannels related to Late Quaternary sea-level changes in southern Brazil. *Brazilian Journal of Oceanography*, **58**:35-44. http://dx.doi.org/10.1590/S1679-87592010000600005

Weschenfelder J., Corrêa I.C.S., Aliotta S., Pereira C.M., Vasconcellos V.E.B. 2006. Shallow gas accumulation in sediments of the Patos Lagoon, Southern Brazil. *Annals of the Brazilian Academy of Sciences*, **78**(3):607-614.

Weschenfelder J., Corrêa I.C.S., Baitelli R., Toldo Jr. E.E. 2010b. A drenagem pretérita do Rio Camaquã na costa do Rio Grande do Sul. *Pesquisas em Geociências*, **37**(1):13-23. https://doi.org/10.22456/1807-9806.17717

Weschenfelder J., Corrêa I.C.S., Toldo Jr. E.E., Baitelli R. 2008a. Paleocanais como indicativo de eventos regressivos quaternários do nível do mar no sul do Brasil. *Revista Brasileira de Geofísica*, **26**(3):367-375. http://dx.doi.org/10.1590/S0102-261X2008000300009

Weschenfelder J., Klein A.H.F., Green A.N., Aliotta S., Mahiques M.M., Ayeres Neto A., Terra L.C., Corrêa I.C.S., Calliari L.J., Montoya I., Ginsberg S.S., Griep G.H. 2016. The control of palaeo-topography in the preservation of shallow gas accumulation: examples from Brazil, Argentina and South Africa. *Estuarine, Coastal and Shelf Science*, **172**:93-107. http://dx.doi.org/10.1016/j.ecss.2016.02.005

Weschenfelder J., Medeanic S., Corrêa I.C.S., Aliotta A. 2008b. Holocene paleoinlet of the Bojuru region, Lagoa dos Patos, southern Brazil. *Journal of Coastal Research*, **24**(1A):99-109. https://doi.org/10.2112/04-0369.1

Zaitlin B.A., Dalrymple R.W., Boyd R. 1994. The stratigraphic organization of incised-valley systems associated with relative sea-level change. *In*: Dalrymple R.W., Boyd R., Zaitlin B.A. (Eds.) *Incised-valley systems: origin and sedimentary sequences*. Tulsa, Oklahoma, SEPM Special Publication. Society for Sedimentary Geology (SEPM), **51**, p. 45-60.

Zenkovitch V.P. 1959. On the genesis of cuspate spits along lagoon shores. *Journal of Geology*, **67**:269-277. https://doi.org/10.1086/626583